

Correlation of the Cd-to-Te ratio on CdTe surfaces with the surface structure

Y. S. Wu,* C. R. Becker, A. Waag, M. M. Kraus, R. N. Bicknell-Tassius, and G. Landwehr
Physikalisches Institut der Universität Würzburg, D-8700 Würzburg, Federal Republic of Germany

(Received 20 November 1990)

We report here that reconstruction on (100), (111)*A*, and (111)*B* CdTe surfaces is either $c(2\times 2)$, (2×2) , and (1×1) or (2×1) , (1×1) , and (1×1) when they are Cd or Te stabilized, respectively. There is a mixed region between Cd and Te stabilization in which the reflected high-energy electron-diffraction (RHEED) patterns contain characteristics of both Cd- and Te-stabilized surfaces. We have also found that the Cd-to-Te ratio of the x-ray photoelectron intensities of their $3d_{3/2}$ core levels is about 20% larger for a Cd-stabilized (111)*A*, (111)*B*, or (100) CdTe surface than for a Te-stabilized one. According to a simple model calculation, which was normalized by means of the photoelectron intensity ratio of a Cd-stabilized (111)*A* and a Te-stabilized (111)*B* CdTe surface, the experimental data for CdTe surfaces can be explained by a linear dependence of the photoelectron-intensity ratio on the fraction of Cd in the uppermost monatomic layer. This surface composition can be correlated with the surface structure, i.e., the corresponding RHEED patterns. This correlation can in turn be employed to determine Te and Cd evaporation rates. The Te reevaporation rate is increasingly slower for the Te-stabilized (111)*A*, (111)*B*, and (100) surfaces, while the opposite is true for Cd from Cd-stabilized (111)*A* and (111)*B* surfaces. In addition, Te is much more easily evaporated from all the investigated surfaces than is Cd, if the substrate is kept at normal molecular-beam-epitaxy growth temperatures ranging from 200 °C to 300 °C.

I. INTRODUCTION

The II-VI semiconductor alloys $\text{Hg}_{1-x}\text{Cd}_x\text{Te}$, $\text{Hg}_{1-x}\text{Mn}_x\text{Te}$, and $\text{Hg}_{1-x}\text{Zn}_x\text{Te}$ are of great interest because of their use in infrared detectors.¹⁻⁶ $\text{Cd}_{1-x}\text{Mn}_x\text{Te}$ and $\text{Cd}_{1-x}\text{Zn}_x\text{Te}$ are also interesting since the former is a widely studied semimagnetic semiconductor and the latter is an extensively used, lattice-matched substrate for Hg-Cd-Te alloys as well as a wide-gap semiconductor with a band gap that ranges from 1.5 to 2.3 eV and thus has a potential as a tunable source, detector, or solar cell in the visible region.⁷⁻¹⁰ The basic substrate materials for molecular-beam-epitaxy (MBE) growth of such alloys are CdTe, $\text{Cd}_{1-x}\text{Zn}_x\text{Te}$, and to a lesser extent GaAs, whose crystalline quality is normally better than that of CdTe and $\text{Cd}_{1-x}\text{Zn}_x\text{Te}$. However, a CdTe buffer is usually grown on the substrate, which must be thicker in the case of GaAs due to the large lattice mismatch. Therefore the MBE growth of high-quality CdTe is of the utmost importance. Consequently many workers²⁻¹⁶ have been involved in an attempt to improve the quality of MBE-grown CdTe- and Hg-based films.

Greater reproducibility in crystalline quality of MBE-grown GaAs has been achieved by correlating the bulk properties of MBE-grown GaAs to the surface stoichiometry.¹¹ The structure of a real surface is always different from the structure of the truncated bulk material due to a rearrangement of the surface atoms. Thus the first layer has a different periodicity, which is strongly correlated to the bulk symmetry and which depends on the growth conditions.

For these reasons we have investigated the influence of various growth conditions on the CdTe surface. The method most widely employed to study the surface during MBE growth is reflection high-energy electron diffraction (RHEED). RHEED patterns can be used to observe surface reconstruction as a function of growth conditions such as source fluxes, substrate temperature, etc.^{2,11-15} However, high-energy electrons (HEE) have been shown to influence the surface appreciably¹⁴ and thus one must be sure that the HEE are not changing what one is studying. To our knowledge, no publication has correlated RHEED patterns to the Cd and Te contents of the uppermost atomic layer or layers. Recently Benson *et al.* proposed that the half-order reconstruction (HOR) in the [011] azimuth is related to a Te-stabilized surface and HOR in the [001] and [010] azimuths is related to a Cd-stabilized surface.¹² In principle, the concentrations of the surface layer or layers can be determined with the help of x-ray photoelectron spectroscopy (XPS). However, there are some experimental difficulties such as uncertainty in the atomic sensitivity factors (ASF).¹⁶⁻²⁰

In this investigation we determined the ratio of the photoelectron intensity of the $3d_{3/2}$ core levels of Cd and Te, corresponding to the RHEED pattern of a (100) CdTe surface ranging from a Cd-stabilized to a Te-stabilized surface. We propose a simple model that is normalized using the results of measurements on the (111)*A* and (111)*B* CdTe surfaces and that allows us to calculate a Cd fraction in the uppermost monatomic layer (Cd surface coverage) and thus to correlate it to a RHEED pattern. XPS measurements have been carried out on (100) and (110) surfaces grown under different conditions.

II. EXPERIMENTAL DETAILS

The experiments were performed using a four-chamber RIBER 2300 MBE system; two growth chambers for wide-band and narrow-band II-VI semiconductors, one XPS chamber, and one metallization chamber. These chambers are connected with each other by means of a transfer system. Normally the vacuum is better than 6×10^{-10} and 2×10^{-9} Torr in the narrow-band growth chamber and transfer system, respectively. The acceleration voltage of the RHEED electron gun was approximately 9 kV, the incident-electron-beam current was between 20 and 80 μA , and the beam was focused as small as possible. XPS experiments were performed with a RIBER MAC2 electron spectrometer using a Mg $K\alpha$ x-ray source ($h\nu = 1235.6$ eV) with an acceleration voltage of 10 kV, a current of 10 mA, and without a monochromator.

The substrates employed were mostly $\text{Cd}_{1-x}\text{Zn}_x\text{Te}$ (4% Zn) and some CdTe with (100), (110), (111)*A*, and (111)*B* orientations. They were chemomechanically polished for several minutes, degreased using standard solvents, etched in a weak solution of bromine in methanol, and rinsed in methanol. Immediately prior to loading the substrates into the MBE system, they were rinsed in deionized water, briefly dipped in hydrochloric acid, and then rinsed in deionized water to remove any remaining carbon and all of the original oxide from the surface. The substrates were preheated at 100°C for 15 min and then the temperature was slowly raised to 340°C–350°C, until the RHEED pattern indicated an absence of oxygen.

In order to obtain a smooth CdTe surface as determined by the RHEED pattern, i.e., long, uniform streaks, and thus a consistent starting point, we first grew a CdTe buffer at 300°C–350°C for 2 h, which was about 1 μm thick. A CdTe flux of 3.5×10^{-7} Torr was used throughout this investigation for the growth of CdTe. The substrate temperature was lowered to 230°C and CdTe was allowed to grow for 1.5 h, with an additional thickness of about 1 μm . In order to obtain a smooth CdTe surface on the (111)*A* surface, a growth temperature of at least 320°C was required. Before a substrate was used again it was heated to 340°C for 10 min and a smooth surface was reestablished by growing a CdTe buffer for about 30 min at 230°C, again with the exception of the (111)*A* surface, which required 340°C. These are the normal starting materials for the experiments described below in the results from Secs. III A–III E, unless otherwise stated.

The substrate was then either kept in a Cd or Te environment in order to produce a Cd- or Te-stabilized surface, or heated to a higher temperature in order to obtain a mixed surface. The Cd and Te environments consisted of Cd and Te fluxes of 2×10^{-7} and 3×10^{-7} Torr, respectively. The only exceptions were a Cd flux of 1×10^{-6} Torr for the (110) surface and a Te flux of 6×10^{-7} Torr for the (111)*A* surface. The photoelectron-intensity ratio (Q) of Cd and Te $3d_{3/2}$ core levels was measured at room temperature using the area of the corresponding peaks with an experimental error of about

1%. The $3d_{3/2}$ core levels were employed rather than the $3d_{5/2}$ core levels in order to avoid the $K\alpha$ satellites of Mg.

III. RESULTS

Throughout this paper we consistently use the convention of referring to the direction of the incident electrons when referring to reconstruction in a particular azimuth. Normally, after preheating the (100) CdTe substrate, RHEED patterns can be observed in the $[0\bar{1}1]$, $[0\bar{1}3]$, $[001]$, $[013]$, $[011]$, $[031]$, $[010]$, and $[03\bar{1}]$ azimuths as shown in Fig. 1 and in the opposite directions. No distinct HOR could be found on such a surface. However, during growth, HOR was observed in some of these azimuths. For normal growth conditions a strong HOR in the (011) azimuth and weak but clear HOR in the $[03\bar{1}]$ azimuth were observed. Reconstruction was present in the $[001]$, $[013]$, $[031]$, and $[010]$ azimuths on a Cd-stabilized surface, and in the $[0\bar{1}1]$, $[0\bar{1}3]$, $[011]$, and $[03\bar{1}]$ azimuths on a Te-stabilized surface. Half-order reconstruction in the $[03\bar{1}]$ azimuth is accompanied by two weaker lines indicating the possibility of a fourfold reconstruction. RHEED observations for (111) CdTe are more complicated and are described below.

A. (100) Te-stabilized surface

In order to get a Te-stabilized CdTe surface we opened the Te shutter immediately after CdTe growth and kept the starting material in a Te environment for about 2 min until the sample temperature was less than 210°C. Whereas HOR was very strong in the $[011]$ azimuth, it was weaker but distinct in the $[0\bar{1}1]$ azimuth. If the reconstruction were pure (2×1) as reported in the literature,^{6,12} the HOR in the $[0\bar{1}1]$ azimuth should be absent instead of weaker. We therefore suggest that either the surface is not completely Te stabilized or the reconstruction is an approximation of (2×1) but will be hereafter designated as (2×1). The strength of HOR in the $[03\bar{1}]$

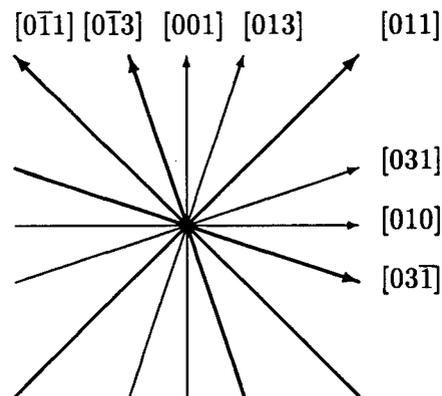


FIG. 1. The azimuths in which reconstruction can be observed in reflection high-energy electron-diffraction patterns of the (100) CdTe surface. The azimuths for a Te and Cd environment are indicated by thick and thin lines, respectively.

azimuth was the same as that of the integral order streaks. It completely disappeared when in a Cd environment and therefore equal HOR and integral order intensities were considered to signify a Te-stabilized surface. At room temperature we found no change in the RHEED pattern. This is consistent with the fact that the desorption time of Te atoms from the surface at 210 °C is at least several hours, according to the measurements of Benson *et al.*¹² and Wu *et al.*^{13,14} From XPS measurements the photoelectron-intensity ratio Q was determined to be 0.430 and is listed in Table I.

B. (100) Cd-stabilized surface

Similarly, a Cd-stabilized surface was established by exposing the starting material to a Cd environment until the substrate temperature was below 180 °C. After closing the Cd shutter and the main shutter, the substrate was held at 180 °C for several minutes, and then cooled to room temperature where the intensity of the HOR between the zero- and first-order Laue zones was the same as that of the HOR between the first- and second-order Laue zones in the [010] azimuth. We used this equality of HOR intensities to signify a Cd-stabilized surface. No HOR was observed in the [03 $\bar{1}$] azimuth. At the present we ignore HOR in the [011] azimuth because it was very weak and could not be completely removed. We attempted to produce HOR in the [010] azimuth without HOR in the [011] azimuth by keeping CdTe at 150 °C in a larger Cd flux. After the RHEED patterns disappeared, which occurred within several seconds, we slowly increased the substrate temperature until HOR appeared in the [010] and [011] azimuths simultaneously.

We have also preheated several CdTe substrates at 350 °C–400 °C for 15 min and then cooled them to 150 °C in a Cd environment. Obviously such substrates should have a very rough surface. Their RHEED patterns were spotty and no reconstruction could be found. But their intensity ratio Q was about 0.50, which is almost the same as that for a smooth Cd-stabilized surface, 0.505.

C. (100) Cd-Te mixed surface

Surfaces intermediate to a Te- and a Cd-stabilized surface, as judged by the RHEED patterns and their intensity ratios obtained from XPS measurements, were ob-

tained by keeping the starting material at a particular temperature without either a Te or Cd flux. The three surfaces that result at temperatures of 340 °C, 280 °C, and 230 °C are considered below and the experimental results are also listed in Table I.

The first surface was acquired by growing CdTe at 340 °C for 20 min and then allowing the sample to cool to room temperature after stopping the growth. HOR between the first- and second-order Laue zones in the [010] azimuth was still strong. HOR in the [03 $\bar{1}$] azimuth was present but very weak. Using a smaller Cd flux at lower temperatures can also produce such a surface structure.

In the second case CdTe was grown for several minutes with the substrate at 280 °C. HOR was weaker between the first- and second-order Laue zones in the [010] azimuth but stronger and clearer in the [03 $\bar{1}$] azimuth than in the first case.

The third surface was that of our normal starting material, i.e., CdTe grown at 230 °C for 30 min and cooled to room temperature after growth. HOR in the [010] azimuth completely disappeared, was very strong in the [011] azimuth, and was very clear in the [03 $\bar{1}$] azimuth. The surface was very smooth as indicated by the uniform streaks in the RHEED pattern.

It is clear from Table I that as the intensity ratio Q decreases, HOR in the [011] azimuth becomes stronger while HOR in the [03 $\bar{1}$] azimuth increases in intensity until it is the same as that of the integral streaks. In contrast, HOR in the [010] azimuth decreases in intensity until it disappears completely. HOR in the [011] azimuth is always present if the surface is smooth enough. Therefore, as mentioned above, HOR intensities in the [03 $\bar{1}$] and [010] azimuths are an indication of Te- and Cd-stabilized surfaces, respectively.

D. (110) CdTe surface

The (110) face is a nonpolar face, as shown in Fig 2. This face is ideally terminated by Cd and Te atoms, each with a single dangling bond at the surface where nucleation and growth occurs. We grew CdTe on the (110) CdTe substrate at a temperature ranging from 150 °C to 350 °C and no reconstruction other than (1×1) was found. The (1×4) reconstruction, as found by Arias, Shin, and Gertner, on (110) Hg_{1-x}Cd_xTe substrates,²¹

TABLE I. The photoelectron-intensity (peak area) ratio Q of the $3d_{3/2}$ core level of Cd and Te atoms in (100) CdTe, as well as the directions in which reconstruction was observed in the reflection high-energy electron-diffraction (RHEED) patterns for different experimental conditions. An asterisk denotes weak but distinct reconstruction.

$Q(\text{Cd:Te})$ Conditions	0.505 Cd stabilized	0.480 $T_s = 340^\circ\text{C}$	0.460 $T_s = 280^\circ\text{C}$	0.440 $T_s = 230^\circ\text{C}$	0.430 Te stabilized
The azimuths in which reconstruction was observed in the RHEED patterns	[010] [001] [013] [031] [011]*	[010] [001] [013] [031] [011]* [03 $\bar{1}$]* [0 $\bar{1}$ 3]*	[010] [001] [013] [031] [011] [03 $\bar{1}$] [0 $\bar{1}$ 3]	[011] [03 $\bar{1}$] [0 $\bar{1}$ 3] [0 $\bar{1}$ 1]*	[011] [03 $\bar{1}$] [0 $\bar{1}$ 3] [0 $\bar{1}$ 1]*

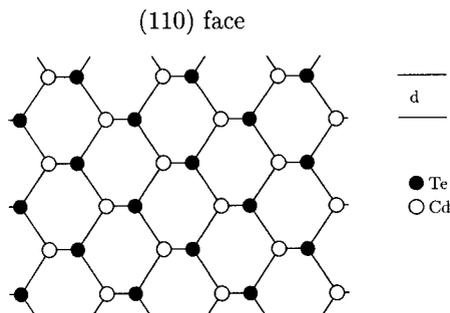


FIG. 2. Crystal structure of (110) CdTe: \circ , Cd; \bullet , Te.

could not be found by either keeping the substrate in a Cd environment at 80°C or in a Te environment at 160°C. An intensity ratio of 0.466 ± 0.005 was obtained using various conditions, such as subjecting the substrate to a Cd or Te environment for several minutes, as long as the RHEED pattern indicated a smooth surface.

E. (111)A and (111)B CdTe surfaces

The (111) face in the zinc-blende structure is a polar face. This polarity leads to two types of faces, as shown in Fig. 3. The first is the (111)A face. It is terminated by either a triply bonded Cd atom or a singly bonded Te atom and is called the Cd face since the stable configuration is terminated by Cd atoms. We grew CdTe at temperatures ranging from 340°C to 200°C but found clear (2×2) reconstruction, which is typical of a CdTe surface in a Cd environment, only during growth at temperatures between 320°C and 340°C. After growth reconstruction became stronger and after 10 h at 230°C in the growth chamber, the HOR strength was the same as that of the integral streaks and the RHEED pattern was smoother. The intensity ratio Q was 0.509 and the RHEED patterns had not changed after the XPS measurement.

However, if kept in a Te environment until the temperature was 120°C or less, reconstruction was (1×1) and the measured Q was 0.402. High-energy electrons reestablished (2×2) reconstruction in a Te environment in a very short time, decreasing to nearly zero at higher substrate temperatures. This behavior was observed at temperatures as low as 70°C. In the absence of HEE and a

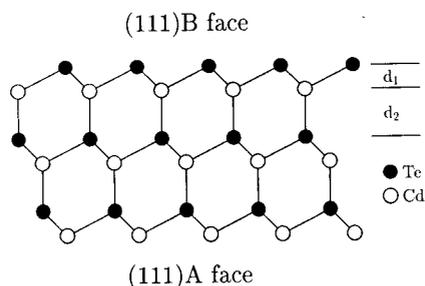


FIG. 3. Crystal structure of (111) CdTe: \circ , Cd; \bullet , Te.

Te environment, (1×1) reconstruction persisted for 10–20 s at 150°C before becoming (2×2). HEE irradiation was avoided, or more precisely limited to a period of 2–3 s, by means of a switch that allowed the x-y deviation voltages of the electron gun to be changed rapidly.

The other possible face, the (111)B face, is terminated by Te atoms.¹⁵ During CdTe growth we observed $(2\sqrt{3} \times 2\sqrt{3})R 30^\circ$ reconstruction, which became stronger after stopping growth, as reported by Sivananthan *et al.*,¹⁵ Hsu *et al.*,¹⁶ and Benson and Summers.²² However, in a Te environment the $(2\sqrt{3} \times 2\sqrt{3})R 30^\circ$ RHEED pattern immediately disappeared and was transformed into a very clear and smooth (1×1) reconstruction if the sample was not being irradiated by HEE. Even though (1×1) reconstruction in a Te environment could be changed to a $(2\sqrt{3} \times 2\sqrt{3})R 30^\circ$ reconstruction in about 10 s after the Te shutter was closed at 230°C, at least 10 min was required in the Cd case at 230°C. This is contrary to what one would expect because the (111)B is normally terminated with Te atoms.

After growing at 230°C for half an hour, the intensity ratio Q ranged from 0.480 to 0.495, increasing with the time that the film was held at a temperature of more than 200°C. In contrast, if the substrate was subjected to a Te environment until being cooled to 150°C or less, which maintained the (1×1) reconstruction, a Q of 0.433 was measured. Even though growth in a Cd environment is more difficult, (1×1) reconstruction was also observed on the (111)B face in a Cd environment, as observed by Benson and Summers.²² Its intensity ratio Q was 0.505. (1×1) reconstruction in a Te environment on both (111)A and (111)B was easily removed by HEE in a matter of seconds. It is obvious that HEE employed in RHEED observations have a large effect on these surfaces. This may be the reason why (1×1) reconstruction has not been reported before.

IV. MODEL FOR THE CALCULATION OF THE Cd FRACTION ON CdTe SURFACES

In this model we assume that a Cd-stabilized (111)A surface and a Te-stabilized (111)B surface are completely covered with one monatomic layer of Cd or Te, respectively. This allows us to calculate a surface ASF ratio for the Cd and Te $3d_{3/2}$ core levels. Using this ratio, the Cd fraction on the (100) and (110) surfaces can be determined. This calculation is described in detail below and the results will be compared with experiment.

In terms of XPS theory, the attenuation of the photoelectron flux through inelastic scattering can be described as follows. If $I_0(x)$ is the photoelectron flux, at a particular electron kinetic energy E , originating at a depth x below the surface of a solid, the flux $I(x)$ emerging from the surface is given by

$$I(x) = I_0(x) \exp \left[\frac{-x}{\lambda} \right], \quad (1)$$

where λ is the mean escape depth of an electron of energy E within the material concerned.

Thus flux, which experimentally is the peak area of the

$3d_{3/2}$ core level of either Cd or Te, is given for a (111)*A* surface by

$$I_{\text{Cd}} = NI_{\text{Cd}}(0) \exp \left[\frac{-d_{\text{Cd}}}{\lambda_{\text{Cd}}} \right] \sum_{n=0}^{\infty} \exp \left[\frac{-n(d_1 + d_2)}{\lambda_{\text{Cd}}} \right]$$

$$= NI_{\text{Cd}}(0) \frac{\exp \left[\frac{-d_{\text{Cd}}}{\lambda_{\text{Cd}}} \right]}{1 - \exp \left[\frac{-d_1 - d_2}{\lambda_{\text{Cd}}} \right]}, \quad (2)$$

$$I_{\text{Te}} = NI_{\text{Te}}(0) \exp \left[\frac{-d_{\text{Cd}} - d_1}{\lambda_{\text{Te}}} \right] \sum_{n=0}^{\infty} \exp \left[\frac{-n(d_1 + d_2)}{\lambda_{\text{Te}}} \right]$$

$$= NI_{\text{Te}}(0) \frac{\exp \left[\frac{-d_{\text{Cd}} - d_1}{\lambda_{\text{Te}}} \right]}{1 - \exp \left[\frac{-d_1 - d_2}{\lambda_{\text{Te}}} \right]}, \quad (3)$$

where $I_{\text{Cd}}(0)$ and $I_{\text{Te}}(0)$ are the photoelectron intensities produced by one Cd and one Te atom, respectively. N is the number of atoms in one monatomic layer, d_1 and d_2 are the distances between neighboring layers and are equal to 0.935 and 2.806 Å, respectively, as shown in Fig. 3, and d_{Cd} is the electron cloud thickness of the top layer, which we assume to be the covalent radius of Cd, 1.48 Å.

The photoelectron-intensity ratio for a Cd-stabilized (111)*A* surface, $Q_{\text{Cd}}[(111)A]$, is then

$$Q_{\text{Cd}}(111)A = \frac{I_{\text{Cd}}}{I_{\text{Te}}}$$

$$= \frac{I_{\text{Cd}}(0)}{I_{\text{Te}}(0)} \left[\frac{1 - \exp \left[\frac{(-d_1 - d_2)}{\lambda_{\text{Te}}} \right]}{1 - \exp \left[\frac{(-d_1 - d_2)}{\lambda_{\text{Cd}}} \right]} \right]$$

$$\times \exp \left[\frac{d_{\text{Cd}} + d_1}{\lambda_{\text{Te}}} - \frac{d_{\text{Cd}}}{\lambda_{\text{Cd}}} \right]. \quad (4)$$

Similarly, for a Te-stabilized surface on the (111)*B* surface,

$$Q_{\text{Te}}(111)B = \frac{I_{\text{Cd}}}{I_{\text{Te}}}$$

$$= \frac{I_{\text{Cd}}(0)}{I_{\text{Te}}(0)} \left[\frac{1 - \exp \left[\frac{(-d_1 - d_2)}{\lambda_{\text{Te}}} \right]}{1 - \exp \left[\frac{(-d_1 - d_2)}{\lambda_{\text{Cd}}} \right]} \right]$$

$$\times \exp \left[\frac{d_{\text{Te}}}{\lambda_{\text{Te}}} - \frac{d_{\text{Te}} + d_1}{\lambda_{\text{Cd}}} \right], \quad (5)$$

where d_{Te} has been taken to be the covalent radius of Te, 1.36 Å.

Equations (4) and (5) contain the factor $I_{\text{Cd}}(0)/I_{\text{Te}}(0)$, which is the ratio of the surface ASF for Cd and Te and which depends upon the instrument and the material. Therefore one would like to eliminate this factor. In order to do this we have divided Eq. (4) by Eq. (5), resulting in

$$R = Q_{\text{Cd}}(111)A / Q_{\text{Te}}(111)B,$$

$$R = \exp[(d_{\text{Te}} - d_{\text{Cd}})(1/\lambda_{\text{Cd}} - 1/\lambda_{\text{Te}})]$$

$$\times \exp[d_1(1/\lambda_{\text{Cd}} + 1/\lambda_{\text{Te}})]. \quad (6)$$

If one uses the atomic radii or even half of the average distance between neighboring atomic layers for d_{Cd} and d_{Te} , both Q and R are changed by less than 0.3%. Values in the literature for the photoelectron escape depth for Cd $3d_{3/2}$ core levels range from 15 to 18 Å.^{23,24} The corresponding value for Te was calculated using the relationship of $\lambda \sim E^{0.75}$.²³ Using this range of values for the escape depths results in an uncertainty in Q and R of $\pm 1\%$ and $\pm 3\%$, respectively.

Assuming this model is correct for Cd- and Te-stabilized surfaces and normalizing it with Cd- and Te-stabilized (111)*A* and (111)*B* surfaces, respectively, i.e., setting the experimental values for $Q_{\text{Cd}}(111)A$ and $Q_{\text{Te}}(111)B$ in Eqs. (4) and (5), the factor $I_{\text{Cd}}(0)/I_{\text{Te}}(0)$ was determined to be 0.395 ± 0.009 . This factor can in turn be used to calculate Q for other Cd- and Te-stabilized surfaces, e.g., $Q_{\text{Cd}}(100)$, $Q_{\text{Te}}(100)$, $Q_{\text{Cd}}(111)B$, and $Q_{\text{Te}}(111)A$, which are listed in Tables I and II along with their experimental values and their photoelectron-intensity ratios.

Furthermore, both the calculated and measured values for R corresponding to the Cd- and Te-stabilized surfaces on (100), (110), (111)*A*, and (111)*B* faces are reproduced in Table III.

It has been established by low-energy electron diffraction (LEED), electron energy-loss spectroscopy (EELS), and theoretical calculations that the (110) surface of CdTe undergoes a (1×1) reconstruction in which the Te atoms at the surface move out by 0.18 Å and the Cd atoms move in by 0.64 Å.^{25,26} Here we have ignored this

TABLE II. Experimental and theoretical values of the photoelectron-intensity (peak area) ratio Q of the $3d_{3/2}$ core level of Cd and Te atoms for Cd- and Te-stabilized (100), (111)*A*, (111)*B*, and (110) CdTe surfaces, e.g., $Q_{\text{Te}}(111)A$ is the Cd to Te intensity ratio of the Te-stabilized (111)*A* surface.

	Experimental	Theoretical
$Q_{\text{Te}}(100)$	0.430 ± 0.005	0.424 ± 0.004
$Q_{\text{Cd}}(100)$	0.505 ± 0.005	0.527 ± 0.005
$Q_{\text{Te}}(111)A$	0.402 ± 0.005	0.393 ± 0.006
$Q_{\text{Cd}}(111)A$	0.509 ± 0.005	0.503 ± 0.006
$Q_{\text{Te}}(111)B$	0.433 ± 0.005	0.438 ± 0.005
$Q_{\text{Cd}}(111)B$	0.505 ± 0.005	0.573 ± 0.010
$Q_{\text{Te}}(110)$	0.466 ± 0.005	0.465 ± 0.001
$Q_{\text{Cd}}(110)$	0.466 ± 0.005	0.466 ± 0.001

TABLE III. The quotient R of the photoelectron-intensity ratio Q of one Cd-stabilized surface to that of a Te-stabilized surface.

	Experimental	Theoretical
$Q_{\text{Cd}}(100)/Q_{\text{Te}}(100)$	1.17 ± 0.02	1.24 ± 0.03
$Q_{\text{Cd}}(111)A/Q_{\text{Te}}(111)B$	1.16 ± 0.02	1.15 ± 0.03
$Q_{\text{Cd}}(111)A/Q_{\text{Te}}(111)A$	1.27 ± 0.02	1.28 ± 0.03
$Q_{\text{Cd}}(111)B/Q_{\text{Te}}(111)B$	1.16 ± 0.02	1.31 ± 0.03
$Q_{\text{Te}}(110)/Q_{\text{Cd}}(110)$	1.00 ± 0.02	1.00 ± 0.01

effect since the photoelectron intensity should not depend upon the position of the atoms on the surface.

The experimental and theoretical values for both Q , the photoelectron-intensity ratio, and R , the ratio of Q for a Cd-stabilized surface to Q for a Te-stabilized surface fit well with the exception of $Q_{\text{Cd}}(111)B$ and of course $Q_{\text{Cd}}(111)B/Q_{\text{Te}}(111)B$, which will be discussed below.

In Fig. 4 the photoelectron-intensity ratio Q for the (100) surface is plotted versus the Cd surface coverage, i.e., the fraction of Cd in the uppermost monatomic layer. Here the theoretical values for a Cd- and Te-stabilized (100) surface are connected by a solid line and the theoretical uncertainties are represented by two dotted lines. The experimental values for Q are represented by circles with error bars. A theoretical Cd surface coverage can be read directly from Fig. 4 for an experimental Q value. Thus the Cd surface coverage is 5% and $78\% \pm 6\%$ for Te- and Cd-stabilized (100) CdTe surfaces, respectively.

Reconstruction in the RHEED patterns for the (100) surface with nearly equal amounts of Cd and Te occurs in all of the above-mentioned directions, which are listed in Table I. This situation is nearly the same as that observed during the growth of conducting CdTe films using

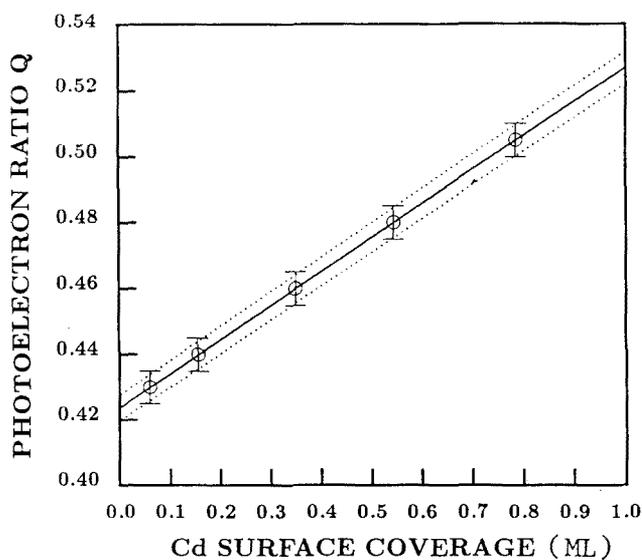


FIG. 4. The theoretical Cd fraction on the (100) CdTe surface vs the photoelectron-intensity ratio as measured by x-ray photoelectron spectroscopy.

excess Cd flux.¹³ According to RHEED, the surface is smooth and displays characteristics of both a Cd- and Te-stabilized surface, i.e., HOR in the [011], [010], and [001] azimuths appear equally strong. This is possible if Cd- and Te-stabilized areas are connected by small steps.

V. DISCUSSION

The growth of high-quality CdTe or $\text{Hg}_{1-x}\text{Cd}_x\text{Te}$ films requires a knowledge of the substrate surface, i.e., concentrations and structure, as determined by methods such as RHEED, XPS, etc. But it is difficult at best to measure the actual surface concentrations. If one uses XPS measurements, then one is confronted with large uncertainties in the atomic sensitivity factors due to differences in XPS instruments and standards.

Lu, Feigelson, and Route studied CdTe (111) surfaces using angle-resolved XPS, Auger electron spectroscopy, and low-energy electron diffraction.¹⁹ They used ASF from the VG ESCALAB handbook to normalize their XPS data and found that Cd and Te compositions on the (111)A and (111)B surfaces were almost the same, $50.0\% \pm 0.5\%$. However, their samples were sputtered using a 1-kV Ar ion beam for 10 min before being annealed at 300°C for 5 min. Obviously these surfaces have been prepared much differently than ours and no comparison should be made.

Hsu *et al.*¹⁶ used thick polycrystalline layers of CdTe, which they proposed to be stoichiometric in order to normalize their XPS measurements of (111)B CdTe. They did not describe the growth conditions under which these layers were grown. However, we have found that polycrystalline CdTe grown on (100) CdTe substrates at room temperature, 130°C , and 160°C have a Te-rich surface, i.e., have a photoelectron-intensity ratio of 0.42 ± 0.01 ; see Fig. 4.

A previous investigation with a RIBER MAC2 electron spectrometer utilized pure Cd and Te on molybdenum in order to normalize the photoelectron intensity of the $3d_{5/2}$ core level of Cd and Te, and thus to obtain an ASF ratio of 0.83.¹⁸ Using this ASF ratio resulted in a Cd-to-Te ratio of 0.69 to 0.51 in a thin CdTe film with a thickness of 38 to 10 Å. Lu, Feigelson, and Route¹⁹ and Ekawa *et al.*²⁰ used an ASF ratio of 0.73 and 0.83, respectively, to normalize their XPS data for $3d_{5/2}$ core levels of Cd and Te on a VG ESCALAB MK II and on a SSX-100, respectively.

In this investigation we have normalized the photoelectron-intensity ratios for the $3d_{3/2}$ core levels by assuming that Cd-stabilized (111)A and Te-stabilized (111)B surfaces are covered by one monatomic layer of Cd and Te, respectively. The experimental and theoretical values of the photoelectron-intensity ratio Q are in good agreement. The only exception is the value of Q for the Cd-stabilized (111)B surface, which can be explained if the singly bonded Cd atoms on the Cd-stabilized (111)B surface have undergone a rearrangement, which is not taken into account by our model. Another possibility is that the surface is not completely Cd stabilized, even with Cd fluxes up to 1×10^{-6} Torr.

Subjecting the (111)B CdTe surface to a large Te flux,

4×10^{-7} Torr, at 210°C resulted in (1×1) reconstruction. According to our XPS measurements the surface was Te stabilized with a photoelectron-intensity ratio Q of 0.433. Benson and Summers observed $(2\sqrt{3} \times 2\sqrt{3})R30^\circ$ but not (1×1) reconstruction on the (111)*B* CdTe surface, probably a result of the higher temperature of 300°C, a much smaller Te flux and possibly the effect of HEE.²²

Because of the good agreement between the experimental and theoretical values of the photoelectron-intensity ratio Q , the surface composition can be correlated with the surface structure, i.e., the corresponding RHEED patterns, as illustrated in Table I. This correlation can in turn be employed to determine Te and Cd evaporation rates as judged by the appropriate changes in the reconstruction.

In this manner we have found that Te reevaporates from a (1×1) Te-stabilized (111)*A* surface very rapidly and indeed faster than from a (111)*B* or (100) surface, i.e., the reevaporation times are 1 s or less, 10 s and 3 h at 230°C, respectively. The reevaporation of Cd from the Cd-stabilized (111)*A* face is much slower than from the Cd-stabilized (111)*B*, i.e., we see no change after 10 h for the former surface as compared to an evaporation time of less than 10 min for the latter surface. Sivananthan *et al.* have reasoned that since the (111)*A* and (111)*B* surfaces are terminated by triply bonded Cd and Te, respectively, Te should act as a cap for Cd and Hg on the (111)*B* surfaces of CdTe and $\text{Hg}_{1-x}\text{Cd}_x\text{Te}$, and thus that Hg and Cd should reevaporate more easily from the (111)*A* surface than from the (111) *B* surface.¹⁵ However, we have observed the opposite behavior for Cd, i.e., according to the RHEED patterns the Cd-stabilized (111)*A* surface remains smooth whereas the Cd-stabilized (111)*B* surface changes in about 10 min. The evaporation rate of Te is much larger than that of Cd, therefore, the evaporation of Cd should be the limiting factor as far as the surface structure is concerned.

VI. CONCLUSIONS

In conclusion we have shown by means of XPS measurements and RHEED observations that CdTe (111)*A*-(2×2), (111)*B*-(1×1) in a Cd environment, and (100)-*c* (2×2) are Cd-stabilized surfaces, and that CdTe (111)*A*-(1×1), (111)*B*-(1×1) in a Te environment, and (100)-(2×1) are Te-stabilized surfaces. There is a mixed region between Cd and Te stabilization in which the RHEED patterns display both Cd- and Te-stabilized surface characteristics, and one is able to obtain a stoichiometric CdTe surface, i.e., the Cd-to-Te ratio in the topmost monolayer is near 1, if the proper fluxes and substrate temperature are employed.

The Cd-to-Te photoelectron-intensity ratio was used to determine the Cd fraction in the uppermost monatomic layer on the surface according to our simple model. Furthermore, the Cd surface coverage was correlated with the surface structure, i.e., the corresponding RHEED patterns. This correlation could in turn be employed to determine Te and Cd evaporation rates. The Te reevaporation rate is increasingly slower for the Te-stabilized (111)*A*, (111)*B*, and (100) surfaces, while the opposite is true for Cd from Cd-stabilized (111)*A* and (111)*B* surfaces.

The Cd-to-Te photoelectron-intensity ratio for the $3d_{3/2}$ core levels, on (100) and (111) surfaces, is about 20% larger for a Cd-stabilized surface than for a Te-stabilized surface, independent of atomic sensitivity factors.

ACKNOWLEDGMENTS

This project was supported by the Bundesministerium für Forschung und Technologie and the Deutsche Forschungsgemeinschaft.

*On leave from Institute of Physics, Chinese Academy of Science, Beijing, China.

¹G. L. Hansen, J. L. Schmitt, and T. N. Casselman, *J. Appl. Phys.* **53**, 7099 (1982).

²S. Sivananthan, M. D. Lange, G. Monfroy, and J. P. Faurie, *J. Vac. Sci. Technol. A* **7**, 788 (1988).

³R. D. Feldman, M. Oran, R. F. Austin, and R. L. Opila, *J. Appl. Phys.* **63**, 2872 (1988).

⁴T. H. Myers, R. W. Yanka, K. A. Harris, A. R. Reisinger, J. Han, S. Hwang, Z. Yang, N. C. Giles, J. W. Cook, Jr., J. F. Schetzina, R. W. Green, and S. McDevitt, *J. Vac. Sci. Technol. A* **7**, 300 (1989).

⁵R. J. Koestner, H.-Y. Liu, H. F. Schaake, and T. R. Hanlon, *J. Vac. Sci. Technol. A* **7**, 517 (1989).

⁶J. P. Faurie, J. Reno, S. Sivananthan, I. K. Sou, X. Chu, M. Boukerche, and P. S. Wijewarnasuriya, *J. Vac. Sci. Technol. B* **6**, 585 (1986).

⁷A. Sher, A.-B. Chen, W. E. Spicer, and C.-K. Shih, *J. Vac. Sci. Technol. A* **3**, 105 (1985).

⁸J. H. Dinan and S. B. Quadri, *J. Vac. Sci. Technol. A* **3**, 851 (1985).

⁹R. D. Feldman, R. F. Austin, A. H. Dayem, and E. H. Westerwick, *Appl. Phys. Lett.* **49**, 797 (1986).

¹⁰G. Lentz, A. Ponchet, N. Magnea, and H. Mariette, *Appl. Phys. Lett.* **55**, 2733 (1989).

¹¹B. A. Joyce, *Rep. Prog. Phys.* **48**, 1637 (1985).

¹²J. D. Benson, B. K. Wagner, A. Torabi, and C. J. Summers, *Appl. Phys. Lett.* **49**, 1034 (1986).

¹³Y. S. Wu, A. Waag, and R. N. Bicknell-Tassius, *Appl. Phys. Lett.* **57**, 1754 (1990).

¹⁴Y. S. Wu, C. R. Becker, A. Waag, R. N. Bicknell-Tassius, and G. Landwehr, *J. Appl. Phys.* **69**, 268 (1991).

¹⁵S. Sivananthan, X. Chu, J. Reno, and J. P. Faurie, *J. Appl. Phys.* **60**, 1359 (1986).

¹⁶C. Hsu, S. Sivananthan, X. Chu, and J. P. Faurie, *Appl. Phys. Lett.* **48**, 908 (1986).

¹⁷A. Waag, Y. S. Wu, R. N. Bicknell-Tassius, and G. Landwehr, *Appl. Phys. Lett.* **54**, 2662 (1989).

- ¹⁸A. Waag, Y. S. Wu, R. N. Bicknell-Tassius, C. Gonser-Buntrock, and G. Landwehr, *J. Appl. Phys.* **68**, 212 (1990).
- ¹⁹Y.-C. Lu, R. S. Feigelson, and R. K. Route, *J. Appl. Phys.* **67**, 2583 (1990).
- ²⁰M. Ekawa, K. Yasuda, S. Sone, Y. Sugiura, M. Saji, and A. Tanaka, *J. Appl. Phys.* **67**, 6865 (1990).
- ²¹J. M. Arias, S. H. Shin, and E. R. Gertner, *J. Cryst. Growth* **86**, 362 (1988).
- ²²J. D. Benson and C. J. Summers, *J. Cryst. Growth* **86**, 354 (1988).
- ²³C. D. Wagner, W. M. Riggs, L. E. Davis, and J. F. Moulder, *Handbook of X-ray Photoelectron Spectroscopy* (Perkin-Elmer, Eden Prairie, MN, 1978); C. J. Powell, *Surf. Sci.* **44**, 29 (1974).
- ²⁴J.-P. Faurie, C. Hsu, and T. M. Duc, *J. Vac. Sci. Technol. A* **5**, 3074 (1987); J. R. Waldrop, R. W. Grant, S. P. Kowalczyk, and E. A. Kraut, *ibid.* **A 3**, 835 (1985).
- ²⁵C. B. Duke, A. Paton, W. K. Ford, A. Kahn, and G. Scott, *Phys. Rev. B* **24**, 3310 (1981).
- ²⁶A. Kahn, *Surf. Sci.* **168**, 1 (1986).